

Supplementary Materials for
**Ventilation of the deep Gulf of Mexico and potential insights to the Atlantic
Meridional Overturning Circulation**

Rainer M.W. Amon *et al.*

Corresponding author: Rainer M.W. Amon, amonr@tamu.edu

Sci. Adv. **9**, eade1685 (2023)
DOI: 10.1126/sciadv.ade1685

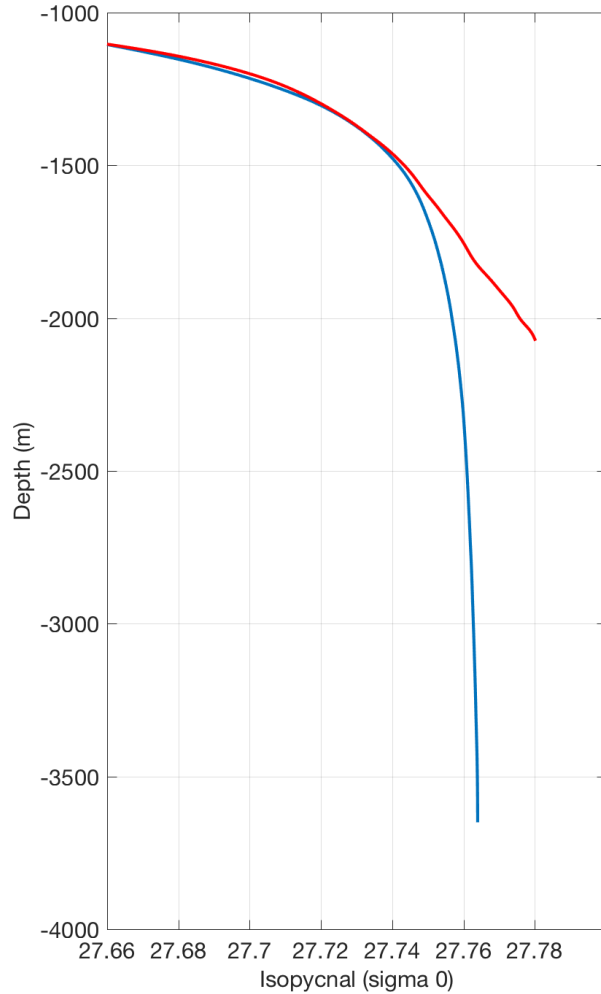
The PDF file includes:

Supplementary Text
Figs. S1 to S6
Tables S1 to S3
Legends for data S1 to S3

Other Supplementary Material for this manuscript includes the following:

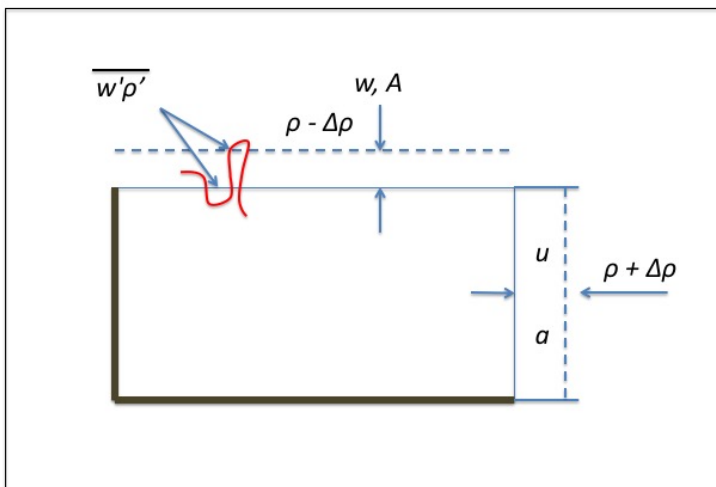
Data S1 to S3

Supplemental Material



Supplemental Figure 1. Mean density (σ_0) profiles at the Yucatan Channel Sill (red) and at the deep interior of the Gulf of Mexico (blue). CTD data are from XIXIMI-6 (2017, blue) and CANEK-42 (2018, red).

Box model for deep GoM residence time calculation



Supplemental Figure 2. Schematic of the box model used to derive residence times from volume transport measurements. Delta rho ($\Delta\rho$) represents an increment in density, rho (ρ) is the density of

the reference volume and rho prime (ρ') represents a density anomaly needed to calculate the turbulent exchange in the upper boundary. U is the horizontal current at Yucatan Channel, a is the cross-sectional area, w is the vertical velocity (upwelling) in the interior of the GoM and A stands for the surface area of a particular isopycnal. The solid line represents the isopycnal that defines the upper boundary of the reference volume. The dashed line is a contiguous isopycnal, with slightly lower density, between which turbulent exchanges are possible. The red curvy line represents those exchanges.

In order to have a ‘model’ from which ‘residence times’ can follow it is necessary to include:

- 1) diapycnal mixing and
- 2) upwelling.

Consider

- i) the inflow of waters heavier than some reference σ_0 (say σ_{0A}),
- ii) the outflow (towards the Caribbean Sea) of same type of waters, and
- iii) the outflow as upwelling through the reference isopycnal surface.

In this model the inflowing waters mix with lighter waters, hence the isopycnal surface is far from a material surface, nonetheless the ‘box’, defined via isopycnals, is well defined, and in this ‘model’ the only inflow is through the Yucatan Channel (red profiles in Fig. 4) and there are two outflows in order for the volume to be conserved and balance the inflow (i.e. a long-term steady density field is assumed). One outflow component is the horizontal current towards the Caribbean Sea (green profiles in Fig 4) and the other outflow component is “diapycnal” upwelling through the reference isopycnal surface.

For the water below a reference density to remain with such density, turbulent exchange with waters above is called for, and the upwelling removes the excess volume that results from the unbalanced horizontal exchange (i.e. along isopycnals) in the Yucatan Channel. The residence time is the time it takes to fill a volume below a certain reference density by the inflow through YC (the same volume is provided by the two outflows). Considering that for this steady state model, mass and volume remain unchanged in the box, there is the compromise for turbulent exchanges to balance the ‘mass excess input’, this does not seem far-fetched as the isopycnal surface in contact with lighter waters is large.

In relation to the schematic model in Supplemental Figure 2:

Conservation of volume in the model domain,

$$\nabla \cdot \underline{u} = 0, \quad ua + wA = 0 \quad (1)$$

where u is the horizontal current at Yucatan Channel, a the cross-sectional area, w the vertical velocity (upwelling) in the interior of the GoM and A stands for the surface area of a particular isopycnal.

Conservation of mass,

$$\frac{\partial}{\partial t} (\rho + \rho') + \nabla \cdot [\rho(\underline{u} + \underline{u}')] = 0$$

where ρ is a reference density and prime quantities are anomalies.

On average this gives:

$$\frac{\partial \rho}{\partial t} + \nabla \cdot \rho \underline{u} + \nabla \cdot \overline{\rho' \underline{u}'} = 0$$

in steady state conditions $\frac{\partial \rho}{\partial t} = 0$, therefore

$$(\rho + \Delta\rho) ua + \rho wA + \overline{\rho'w'A} = 0 \quad (2)$$

$$(1) \ \& \ (2) \Rightarrow \Delta\rho ua + \overline{\rho'w'A} = 0 \quad (3)$$

The *excess* inflowing mass ($\Delta\rho ua$) is released via turbulent mixing ($\overline{\rho'w'A}$) plus mass outflow. The turbulent vertical interchange ($\overline{\rho'w'A}$) does not contribute to the upwelling, the upwelling is w in equation (1).

The net mass transport associated with the volume transport ua is made up of INFLOW (say $\rho_1 u_1 a_1$) and outflow towards the Caribbean Sea ($\rho_2 u_2 a_2$), i.e., $(\rho + \Delta\rho) ua = \rho_1 u_1 a_1 + \rho_2 u_2 a_2$ where in Figure 4 $u_1 a_1$ and $u_2 a_2$ corresponds to the red trace and green traces respectively.

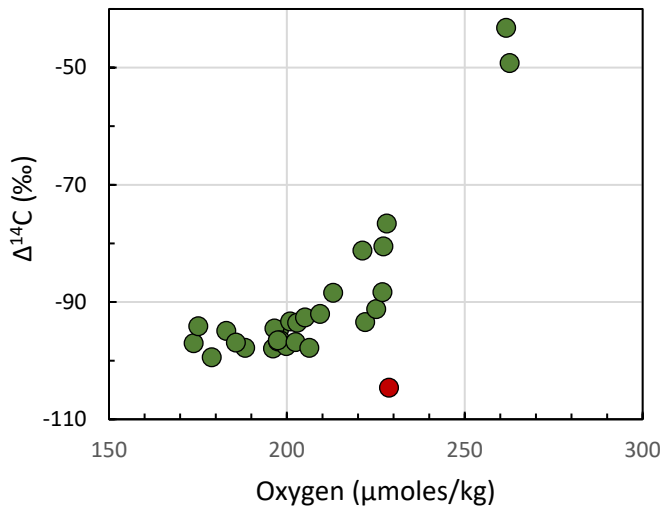
The residence time is therefore the amount of time that transport $u_1 a_1$ (inflowing transport) takes to fill the volume below a given isopycnal. This time is the same as the time it takes for $u_2 a_2 + wA$ to release the same volume, i.e. $u_1 a_1 + u_2 a_2 + wA = 0$

Once this ‘model’ is assumed, residence times can be computed (as shown in Figure 6, main text; also see Ochoa et al. 2021 (26) for a related discussion).

Ventilation of the Venezuelan Basin

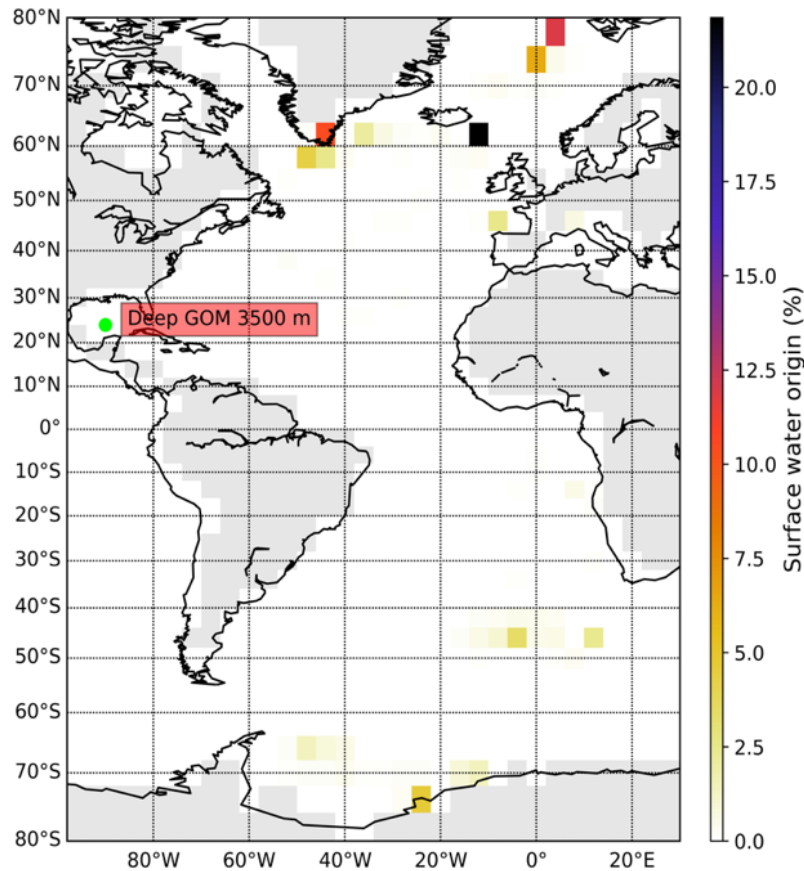
Earlier work suggested a residence time of 540 years (98) and 55 years (85), respectively, for the deep Venezuela Basin (>2500m). The large difference of these estimates is based on the inclusion of entrainment in one of the estimates (98) and a low volume transport of 0.1 Sv through the double sill in the Anegada-Jungfern Passage Complex (85). The $\Delta^{14}\text{C}$ offset of $\sim 18\text{‰}$ between NADW ($\sim 1800\text{m}$) and the deep waters in the Venezuela Basin (85) is similar to the 15‰ difference reported here (main text, Table 1). The dissolved oxygen distribution suggests that the Venezuela Basin cannot be solely ventilated through the Anegada-Jungfern Passage on a timescale of 540 or 55 years (98, 85) because the DO concentrations in the deep basin are either too low or too high. Considering that the DO concentration of inflowing NADW is around 260 μM and assuming an average oxygen consumption in deep waters around 0.15 $\mu\text{M yr}^{-1}$ for UNADW (99) then deep water with an average residence time of 540/55 years should have DO concentrations closer to 180/250 μM , but not the 215 μM observed in the deep Venezuela Basin (Figure 7a). This indicates a different residence time for deep waters in the Venezuela Basin and/or deep-water exchanges with the Cayman Basin through the Colombian Basin. DO concentrations and the radiocarbon content in the different deep basins suggest that the residence time of the deep Venezuelan Basin should be between the values proposed for the Yucatan Basin (~ 45 years) and the GoM (~ 100 years). Assuming a linear relationship between DO concentrations, radiocarbon values and residence times, the waters of the deep Venezuelan Basin should be replaced about every 70-80 years on average.

Relationship of radiocarbon and dissolved oxygen



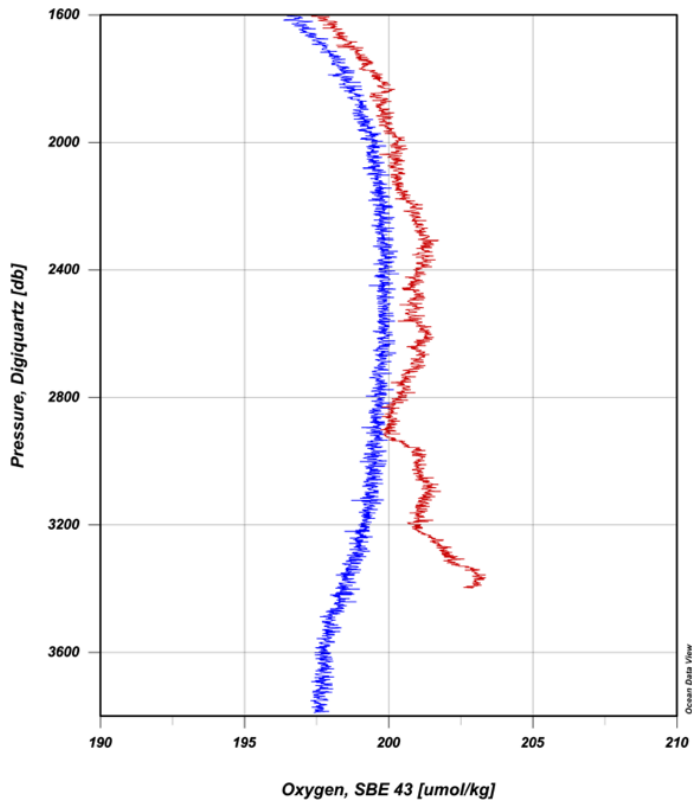
Supplemental Figure 3: Relationship between dissolved oxygen concentrations and radiocarbon in deep waters of the GoM, the Caribbean and the North Atlantic (near Anegada-Jungfern Passage). The red dot represents the 3000 m sample from the 1978 radiocarbon profile (36).

Output from the Total Matrix Intercomparison based on WOCE data

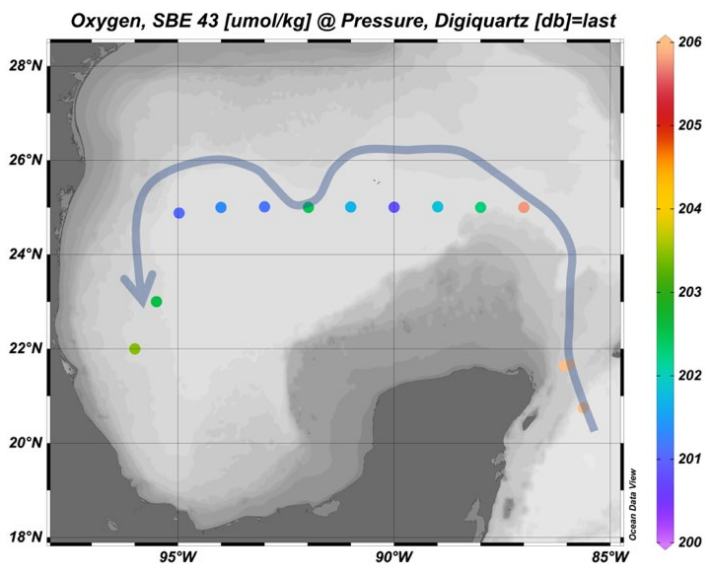


Supplemental Figure 4: Results of the Total Matrix Intercomparison (TMI) method indicating the major surface water sources of deep waters (3500m) in the GoM.

Dissolved Oxygen profiles and bottom distribution in the Gulf of Mexico



Supplemental Figure 5: Oxygen depth profiles (1600m-bottom) at station A10 (easternmost station in the GoM in red) showing intrusions of high oxygen waters from the Yucatan Channel at different depth levels, and at a station in the central GoM (blue) showing a mid-depth DO maximum and general DO decline towards the bottom.



Supplemental Figure 6: Bottom water oxygen distribution during XIXIMI-7, 2019 suggesting a cyclonic bottom water flow from the Yucatan Strait sill towards the north to the Sigsbee Escarpment following the topography to the west and ultimately to the south consistent with bottom water flows (gray arrow). All stations are deeper than 3000m except Yucatan Strait.

Supplemental Table 1. Water mass characteristics (TEOS-10)

Water mass within the GoM	Common abbreviation	Density σ_θ (kg/m ³)	Pot. Temp. °C	Salinity S_A	Depth Range (m)
Surface waters – Gulf Common Water, Caribbean SW	SW GCW, CSW	24.0-26.30 <22.90	20.00-22.50 22.00-28.00	<36.80 <36.70	<150
Subtropical underwater	SUW	25.43-25.68	20.00-25.00	>36.80	150-250
Eighteen-degree water	18°C water	26.20-26.65	17.00-19.00	36.20-36.70	105-320
North Atlantic Central Water	NACW	26.70-26.96	8.58-14.30	35.22-36.00	300-560
South Atlantic Central Water	SACW	26.96-27.34	6.95-8.55	35.10-35.22	560-700
Antarctic Intermediate Water	AAIW	27.38-27.45	5.50-6.50	35.05-35.10	740-900
Upper North Atlantic Deep water	UNADW	>27.76	<4.60	>35.12	>1200

Supplemental Table 2. CMIP6 GCM ensemble and its references and data parameters

Model	reference	experiment id	member id	deep GOM (z)	(m)
CanESM5	Swart et al., 2019 (89)	historical, ssp585	r1i1p1f1	29	2054
CNRM-ESM2-1	Séférian et al., 2016 (90)	historical, ssp585	r1i1p1f2	53	1945
GFDL-CM4	Held et al., 2019 (91)	historical, ssp585	r1i1p1f1	25	2000
GFDL-ESM4	Dunne et al., 2020 (92)	historical, ssp585	r1i1p1f1	25	2062
IPSL-CM6A-LR	Boucher et al., 2020 (93)	historical, ssp585	r1i1p1f1	53	1945
MIROC-ES2L	Hajima et al., 2020 (94)	historical, ssp585	r1i1p1f2	46	1990
MPI-ESM1-2-HR	Müller et al., 2018 (95); Mauritsen et al., 2019 (96)	historical, ssp585	r2i1p1f1	29	2080
MRI-ESM2-0	Yukimoto et al., 2019 (97)	historical, ssp585	r1i2p1f1	47	2000

Supplemental Table 3. Station location and depth of radiocarbon samples (DIC) along with hydrographic data, nutrients, dissolved inorganic carbon (DIC) and alkalinity.

Station	Longitude °W	Latitude °N	Depth m	Date	θ °C	Salinity	σ_θ kg m ⁻³	Nitrate μ moles kg ⁻¹	Silicate μ moles kg ⁻¹	A_T	DIC μ moles kg ⁻¹	DO μ moles kg ⁻¹	$\Delta^{14}C$ ‰
C23	93.000	23.000	10	09/02/2017	29.98	36.62	22.947	0.50	1.90	2390	2051	190.05	43.63
C23	93.000	23.000	50	09/02/2017	26.83	36.48	23.887	0.10	1.50	2391	2055	218.97	40.78
C23	93.000	23.000	102	09/02/2017	23.32	36.35	24.865	0.20	1.60	2455	2098	191.49	44.22
C23	93.000	23.000	150	09/02/2017	20.75	36.58	25.766	5.80	3.30	2388	2159	126.30	53.75
C23	93.000	23.000	445	09/02/2017	10.11	35.242	27.127	20.07	12.79	2304	2208	104.83	-9.64
C23	93.000	23.000	600	09/02/2017	7.87	34.995	27.292	24.07	19.04	2302	2208	112.59	-55.81
C23	93.000	23.000	800	09/02/2017	6.1	34.916	27.479	22.47	23.13	2313	2218	138.19	-86.16
C23	93.000	23.000	1200	09/02/2017	4.52	34.95	27.699	24.00	24.76	2296	2198	185.66	-94.94
C23	93.000	23.000	2500	09/02/2017	4.09	34.98	27.762	22.39	25.41	2326	2191	202.99	-97.53
C23	93.000	23.000	3731	09/02/2017	4.07	34.98	27.765	22.31	25.41	2336	2193	200.65	-96.46
F37	95.000	21.000	50	08/29/2017	27.75	36.47	23.582	0	1.90	2391	2062	215.21	41.23
F37	95.000	21.000	88	08/29/2017	22.78	36.40	25.059	0	1.70	2392	2106	177.78	46.01
F37	95.000	21.000	150	08/29/2017	19.01	36.50	26.168	12.70	4.40	2372	2179	113.93	57.89
F37	95.000	21.000	399	08/29/2017	10.28	35.282	27.114	26.71	14.07	2301	2211	104.29	-6.92

F37	95.000	21.000	600	08/29/2017	7.67	34.978	27.313	15.99	10.25	2337	2172	115.13	-6.47
F37	95.000	21.000	800	08/29/2017	5.93	34.916	27.502	28.69	23.81	2300	2218	143.56	-87.09
F37	95.000	21.000	1200	08/29/2017	4.38	34.96	27.720	24.08	25.27	2331	2206	191.65	-97.75
F37	95.000	21.000	3165	08/29/2017	4.07	34.98	27.765	22.36	25.17	2327	2189	201.48	-96.18
A10	87.051	24.921	10	09/07/2017	30.22	36.34	22.657	0	1.50	2360	2027	191.54	38.48
A10	87.051	24.921	50	09/07/2017	29.23	36.24	22.922	0	1.30	2355	2023	202.40	37.85
A10	87.051	24.921	114	09/07/2017	26.92	36.43	23.823	0	1.30	2357	2056	198.25	41.05
A10	87.051	24.921	150	09/07/2017	26.06	36.67	24.266	NA	NA	NA	NA	178.16	54.99
A10	87.051	24.921	344	09/07/2017	17.52	36.434	26.445	8.19	2.75	2386	2152	155.81	27.14
A10	87.051	24.921	600	09/07/2017	9.46	35.156	27.005	11.01	5.68	2353	2157	121.72	60.51
A10	87.051	24.921	800	09/07/2017	7.91	34.970	27.265	28.18	17.80	2314	2216	116.12	-45.37
A10	87.051	24.921	1200	09/07/2017	4.77	34.95	27.647	25.84	25.07	2321	2208	174.60	-94.07
A10	87.051	24.921	2500	09/07/2017	4.08	34.98	27.764	21.91	23.88	2319	2196	204.09	-93.31
A10	87.051	24.921	3350	09/07/2017	4.07	34.98	27.767	22.13	23.33	2328	2189	206.23	-93.49
Y7	85.944	21.670	10	09/06/2017	29.74	36.19	22.707	0.90	2.90	2363	2014	192.09	39.00
Y7	85.944	21.670	50	09/06/2017	28.95	36.32	23.076	0	1.40	2330	2031	198.95	39.61
Y7	85.944	21.670	90	09/06/2017	27.22	36.49	23.770	0	1.30	2377	2058	197.16	41.66
Y7	85.944	21.670	150	09/06/2017	23.42	36.96	25.300	2.60	1.40	NA	2128	161.25	50.09
Y7	85.944	21.670	450	09/06/2017	12.12	35.524	26.934	20.49	9.07	2336	2210	127.79	26.46
Y7	85.944	21.670	600	09/06/2017	9.22	35.090	27.146	27.40	15.37	2314	2188	116.78	-52.76
Y7	85.944	21.670	800	09/06/2017	6.45	34.857	27.378	28.32	21.13	2290	2208	131.34	-73.77
Y7	85.944	21.670	1000	09/06/2017	4.97	34.93	27.622	26.04	23.98	2315	2204	172.85	-91.32
Y7	85.944	21.670	1200	09/06/2017	4.47	34.96	27.705	23.9	24.56	2327	2196	190.98	-94.39
Y7	85.944	21.670	1892	09/06/2017	4.11	34.98	27.760	22.26	23.41	2326	2186	208.45	-92.63
Y9	85.621	20.916	50	09/06/2017	29.32	36.27	22.915	0.10	1.50	2367	2024	193.51	40.66
Y9	85.621	20.916	99	09/06/2017	27.40	36.47	23.700	0.10	1.30	2379	NA	194.84	40.26
Y9	85.621	20.916	150	09/06/2017	25.20	36.85	24.678	NA	NA	NA	2048	176.43	49.91
Y9	85.621	20.916	319	09/06/2017	17.93	36.49	26.433	9.70	3.30	NA	NA	150.17	57.55
Y9	85.621	20.916	600	09/06/2017	9.46	35.125	27.090	28.10	16.12	2317	2207	118.04	-24.60
Y9	85.621	20.916	842	09/06/2017	6.52	34.869	27.374	29.44	22.16	2307	2209	131.46	-73.73
Y9	85.621	20.916	1200	09/06/2017	4.64	34.95	27.683	24.36	24.04	2305	2196	187.54	-96.91
Y9	85.621	20.916	2000	09/06/2017	4.08	34.99	27.771	20.59	18.8	2316	2175	224.44	-81.15
Y9	85.621	20.916	2500	09/06/2017	3.97	34.99	27.784	18.8	16.14	2322	2170	232.19	-76.57
Y9	85.621	20.916	3100	09/06/2017	3.92	34.99	27.788	18.13	16.69	2324	2167	231.12	-80.47
E1	94.766	23.960	20	04/24/2017	25.49	36.42	24.263	NA	NA	NA	NA	198.94	39.27
E1	94.766	23.960	100	04/24/2017	22.87	36.31	24.971	NA	NA	NA	NA	189.44	39.47
E1	94.766	23.960	150	04/24/2017	20.76	36.62	25.801	NA	NA	NA	NA	127.24	54.89
E1	94.766	23.960	330	04/24/2017	12.71	35.58	26.903	NA	NA	NA	NA	105.94	26.64
E1	94.766	23.960	450	04/24/2017	10.27	35.24	27.095	NA	NA	NA	NA	101.89	-6.68
E1	94.766	23.960	510	04/24/2017	9.25	35.28	27.172	NA	NA	NA	NA	102.99	-25.42
E1	94.766	23.960	810	04/24/2017	6.09	35.08	27.475	NA	NA	NA	NA	135.02	-85.50
E1	94.766	23.960	1200	04/24/2017	4.54	34.95	27.693	NA	NA	NA	NA	179.77	-99.36
E1	94.766	23.960	2500	04/24/2017	4.09	34.98	27.762	NA	NA	NA	NA	197.97	-94.84
E1	94.766	23.960	3600	04/24/2017	4.08	34.98	27.766	NA	NA	NA	NA	196.05	-97.95
E13	94.378	24.923	50	04/27/2017	25.00	36.43	24.427	NA	NA	NA	NA	197.75	43.33
E13	94.378	24.923	125	04/27/2017	24.43	36.42	24.591	NA	NA	NA	NA	190.34	40.25
E13	94.378	24.923	200	04/27/2017	20.37	36.55	25.851	NA	NA	NA	NA	121.52	52.98
E13	94.378	24.923	390	04/27/2017	12.62	35.56	26.909	NA	NA	NA	NA	105.90	26.04
E13	94.378	24.923	500	04/27/2017	10.13	35.22	27.110	NA	NA	NA	NA	102.08	-8.74
E13	94.378	24.923	600	04/27/2017	8.94	35.07	27.188	NA	NA	NA	NA	104.15	-33.69
E13	94.378	24.923	840	04/27/2017	6.26	34.9	27.449	NA	NA	NA	NA	131.36	-81.26
E13	94.378	24.923	1200	04/27/2017	4.68	34.94	27.671	NA	NA	NA	NA	173.76	-97.02
E13	94.378	24.923	2500	04/27/2017	4.09	34.97	27.761	NA	NA	NA	NA	197.47	-96.73
E13	94.378	24.923	3600	04/27/2017	4.08	34.98	27.766	NA	NA	NA	NA	196.48	-94.46
A10	87.002	25.000	10	06/02/2019	28.62	36.24	23.12	0.04	1.57	2335	2034.5	193.63	33.1
A10	87.002	25.000	50	06/02/2019	28.30	36.23	23.224	0.02	1.57	2334	2044.5	194.75	32.4
A10	87.002	25.000	120	06/02/2019	26.54	36.39	23.916	0.10	1.36	2363	2054.2	184.66	32.6
A10	87.002	25.000	150	06/02/2019	26.19	36.49	24.102	0.85	1.34	2388	2082.2	178.97	38.5
A10	87.002	25.000	240	06/02/2019	22.35	36.91	25.575	4.40	1.74	2398	2222.5	156.35	43.7
A10	87.002	25.000	345	06/02/2019	18.05	36.50	26.416	10.11	3.43	2383	2208.4	148.92	53.0
A10	87.002	25.000	500	06/02/2019	13.52	35.75	26.872	29.72	18.61	2310	2219.7	124.16	31.6
A10	87.002	25.000	600	06/02/2019	11.04	35.36	27.054	19.22	8.13	2337	2211	117.16	5.3
A10	87.002	25.000	726	06/02/2019	8.48	35.03	27.228	24.90	12.55	2321	2216.9	113.33	-41.2
A10	87.002	25.000	800	06/02/2019	7.45	34.94	27.312	30.50	21.13	2310	2224	118.71	-63.4
A10	87.002	25.000	883	06/02/2019	6.48	34.91	27.423	28.15	24.49	2317	2225.6	132.02	-78.1
A10	87.002	25.000	1000	06/02/2019	5.78	34.92	27.52	29.53	23.02	2309	2222.5	147.31	-90.2
A10	87.002	25.000	1110	06/02/2019	5.18	34.94	27.607	26.90	25.31	2284	2230.1	164.16	-91.3
A10	87.002	25.000	1200	06/02/2019	4.82	34.95	27.661	26.02	25.59	2317	2225.6	147.93	-96.8
A10	87.002	25.000	1617	06/02/2019	4.22	34.97	27.747	23.27	25.15	2330	2195	200.17	-95.9
A10	87.002	25.000	1820	06/02/2019	4.16	34.98	27.755	22.95	25.06	2330	2196	202.85	-97.5
A10	87.002	25.000	2023	06/02/2019	4.13	34.98	27.760	17.66	20.08	2330	2196	204.18	-95.3
A10	87.002	25.000	2531	06/02/2019	4.09	34.98	27.765	22.40	24.83	2328	2195.9	205.41	-93.1
A10	87.002	25.000	3041	06/02/2019	4.08	34.98	27.768	22.06	24.44	2325	2189	205.86	-92.8
A10	87.002	25.000	3302	06/02/2019	4.08	34.98	27.769	21.96	24.20	2320	2189	206.77	-96
Y9	85.626	20.753	10	06/04/2019	28.95	36.2	22.985	0	1.64	2367	2037	193.37	29.6
Y9	85.626	20.753	50	06/04/2019	27.86	36.12	23.289	0	1.57	2339	2058	203.13	33.6
Y9	85.626	20.753	150	06/04/2019	26.37	36.39	23.969	0.25	1.36	2363	2154	181.2	36.4
Y9	85.626	20.753	235	06/04/2019	24.92	36.79	24.719	3.42	1.59	2283	2171	170.31	42.1

Y9	85.626	20.753	372	06/04/2019	19.23	36.65	26.23	7.69	2.64	2357	2168	153.69	55.7
Y9	85.626	20.753	400	06/04/2019	17.11	36.37	26.542	9.65	3.35	2365	2157	153.17	55.8
Y9	85.626	20.753	495	06/04/2019	13.96	35.80	26.819	17.39	7.28	2303	2153	126.29	38.0
Y9	85.626	20.753	598	06/04/2019	11.62	35.44	27.005	22.50	11.1	2315	2180	119.29	13.4
Y9	85.626	20.753	698	06/04/2019	10.62	35.29	27.077	26.47	15.2	2282	2198	117.03	-20.2
Y9	85.626	20.753	705	06/04/2019	9.80	35.18	27.130	26.77	15.7	2303	2173	115.95	-16.8
Y9	85.626	20.753	807	06/04/2019	7.96	34.95	27.249	29.29	19.8	2304	2198	117.99	-48.0
Y9	85.626	20.753	848	06/04/2019	7.38	34.91	27.301	30.09	23.1	2395	2172	122.29	-74.7
Y9	85.626	20.753	1009	06/04/2019	5.71	34.89	27.509	27.91	24	2298	2209	151.65	-85.4
Y9	85.626	20.753	1110	06/04/2019	5.08	34.94	27.619	25.64	24.6			173.19	-92.6
Y9	85.626	20.753	1211	06/04/2019	4.73	34.96	27.674	24.17	24.60	2312	2212.7	181.73	-93.1
Y9	85.626	20.753	1515	06/04/2019	4.30	34.98	27.738	22.27	23.35	2309	2207.2	203.96	-90.6
Y9	85.626	20.753	1795	06/04/2019	4.16	34.99	27.761	20.58	20.47	2316	2201.1	214.06	-81
Y9	85.626	20.753	1921	06/04/2019	4.10	34.99	27.770	20.75	20.52	2309	2193.4	218.24	-85
Y9	85.626	20.753	2030	06/04/2019	4.06	34.99	27.777	20.36	19.48	2327	2191.9	220.67	-78.6
Y9	85.626	20.753	2150	06/04/2019	4.04	35.00	27.781	19.86	17.85	2301	2178.5	228.18	-73.3
Y9	85.626	20.753	2610	06/04/2019	3.95	34.99	27.789	19.76	17.56	2306	2177.4	231.60	-76.4
Y9	85.626	20.753	4350	06/04/2019	3.91	34.99	27.790	19.84	18.13	2330	2172.6	229.03	-84

Captions for data files:

Data S1 and S2: Volume transport and residence times shown in Figure 5:

A matlab (trademark <https://www.mathworks.com>) data file (physical_data_restimes.mat) and a matlab script (compute_restimes.m) are included as supplementary data to reproduce Figure 5 from the main manuscript. A README_FIG5.txt is also included explaining the contents of the data file. The files contain all the information required to reproduce the Figure including two estimates of the mean (normal to the section) velocity structure based on: (1) the mean of an objectively analyzed velocity field produced by matching transports at Yucatan Channel and Florida Straits and another (2) computed using mean values based on series longer than one year (see 27 for details). It also contains mean vertical profiles of temperature, salinity and potential density for the Yucatan Channel and interior of the Gulf of Mexico and estimates of volumes and areas below certain depths within the Gulf of Mexico (see the README_FIG5.txt for the rest of its contents). The matlab script shows how the calculations to estimate transports and residence times were carried out. The results of these calculations are also included in the data file.

Data S3: Hydrographic data shown in Figure 6:

The file “hydrographic_data” includes the CTD and dissolved oxygen data collected during two research cruises in the Gulf of Mexico and Yucatan Channel on the Mexican R/V Justus Sierra. The XIXIMI-6 cruise was conducted in August 2017 and the XIXIMI-7 cruise was conducted in May 2019. These data are shown in Figure 6 along with the data from the CLIVAR section A22 in 2012 (56).